AIP Conference Proceedings

On the plastic flow localization of martensitic stainless steel saturated with hydrogen

Svetlana Barannikova, Anna Bochkareva, Alexey Lunev, Galina Shlyakhova, Yulia Li, and Lev Zuev

Citation: AIP Conference Proceedings **1783**, 020011 (2016); doi: 10.1063/1.4966304

View online: http://dx.doi.org/10.1063/1.4966304

View Table of Contents: http://scitation.aip.org/content/aip/proceeding/aipcp/1783?ver=pdfcov

Published by the AIP Publishing

On the Plastic Flow Localization of Martensitic Stainless Steel Saturated with Hydrogen

Svetlana Barannikova[1,2,a)], Anna Bochkareva[1,3,b)], Alexey Lunev[1,3,c)], Galina Shlyakhova[1,2,4,d)], Yulia Li[1,2,e)], and Lev Zuev[1,2,f)]

[1] *Institute of Strength Physics and Materials Science SB RAS, Tomsk, 634055 Russia*
[2] *National Research Tomsk State University, Tomsk, 634050 Russia*
[3] *National Research Tomsk Polytechnic University, Tomsk, 634050 Russian*
[4] *Seversk State Technological Institute (National Research Nuclear University MEPhI), Seversk, 636036 Russia*

[a)] bsa@ispms.tsc.ru
[b)] Corresponding author: avb@ispms.tsc.ru
[c)] agl@ispms.tsc.ru
[d)] shgv@ispms.tsc.ru
[e)] jul2207@mail.ru
[f)] lbz@ispms.tsc.ru

Abstract. The deformation behavior of tensile tested corrosion resistant high-chromium steel electrically saturated with hydrogen has been investigated. The studies were performed for high-temperature tempered steel with sorbitic structure and after electrolytic hydrogenation for 6 and 12 hours. It was found that hydrogen has markedly reduced the breaking stress and elongation leading to the fracture of the specimen. Using the method of double-exposed speckle photography, it was found that the plastic flow of the material had localized character. The evolution of localized-strain center distributions follows the law of plastic flow. The autowave parameters (autowave velocity and autowave length) were measured for every state of high-chromium steel under investigation and the difference between them is of great significance.

INTRODUCTION

Over the recent years, we have found experimentally for a range of metals and alloys that plastic deformation at all its stages is prone to localization. The observed localization patterns have wave-like character; the kind of wave depends on the acting law of work hardening, that is, the form of function $\theta(\varepsilon)$ [1, 2]. There are only four of them: single deformation fronts move at the easy glide stage for single crystals and in a yield plateau for polycrystals; a system of equidistant mobile localized-strain centers in the linear hardening stage; spatial periodic structure of plastic strain localization regions at the Taylor parabolic work hardening stage; and the last one is the structure of nonuniform mobile strain localization regions peculiar to the final (prefracture) deformation stage. The objective of this work is to study the interstitial hydrogen atoms impact on the wave parameters for predicting the deformation behavior of engineering materials operating in corrosive media such as water vapor, aquatic and acid environments. For instance, chemical reactors or oil and gas equipment made of high-chromium stainless steel operate in the presence of severe atmosphere of hydrogen. The presence of hydrogen (H) in solid solutions in metals and alloys relates mainly to the small diameter of this element and its capacity to diffuse with certain ease in solid state. Different factors contribute to elevated or diminished solubilization and/or diffusion of hydrogen in steels. The main ones are temperature, alloy composition, crystalline structure and substructure. Nevertheless, the presence of hydrogen in metals—and specifically in steels—is not desired in most cases, since H alters considerably the mechanical and metallurgical properties of these materials potentially leading to a fracture [3–7].

Advanced Materials with Hierarchical Structure for New Technologies and Reliable Structures 2016
AIP Conf. Proc. 1783, 020011-1–020011-4; doi: 10.1063/1.4966304
Published by AIP Publishing. 978-0-7354-1445-7/$30.00

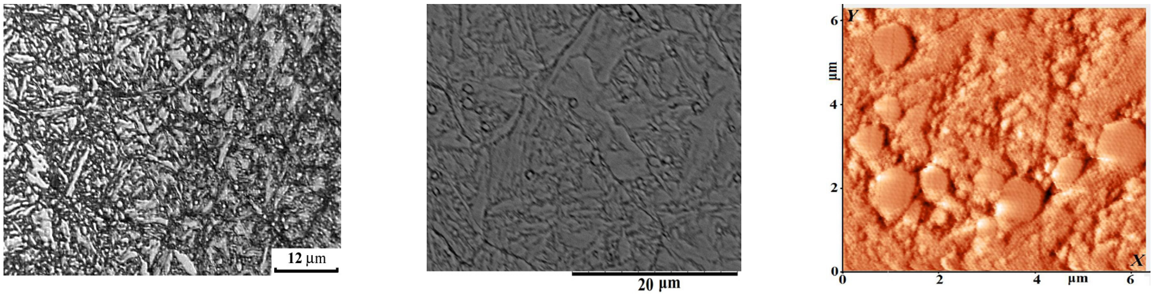

(a) (b) (c)

FIGURE 1. Microstructure images of high-chromium steel in tempered state: (a) optical microscopy, (b) scanning microscopy, (c) atomic-force microscopy; 6.0×6.0 μm section

Such surveys of the localized-strain pattern features for the high-chromium stainless steels widely used in water-vapor, aquatic and acid environments give more information about the behavior of a material comprising a critical structure. The main aim of this investigation was to elucidate the effect of dissolved hydrogen on the macroscopic plastic flow localization patterns in tensile-strained stainless steel polycrystals.

EXPERIMENTAL PART

The investigation was performed for the test samples of high-chromium stainless steel (0.4% C – 0.6% Si – 0.55% Mn – 12.5% Cr). The test samples having dog-bone shape with gage section of $50 \times 10 \times 2$ mm were cut out from sheet steel along the rolling direction. After annealing at $T = 1320$ K for 3 hours with fast air-cooling, this steel has good corrosion resistance due to homogenization via dissolution of intergranular carbides. For the structural metal this steel should be tempered at $T = 873$ K for 3 hours and furnace cooling to increase the plasticity [8, 9]. Determination of steel structural components was performed with a wide set of modern equipment matching the level of advanced technologies in materials science: optical microscope (Neophot-21), scanning microscope (Hitachi TM-1000), atomic force microscope (Solver PH47-PRO, "Nanotechnology-MDT", Zelenograd, Russia) with different types of cantilevers that allow observing various structural features on the studied surfaces. With such heat treatment the ferrite-carbide mixture with small amount of $Me_{23}C_6$-carbides is formed (Fig. 1). Carbide particles are of round or slightly elongated shape, and their size does not exceed 1 μm.

The specimens thus prepared were subjected to electrolytic hydrogenation during 6 and 12 hours under a controlled cathode potential. The sample was placed in a three-electrode electrochemical cell containing 0.1 N sulfuric acid solution heated to the temperature of 323 K. To enhance the process, 20 mg/l of thiocarbonic acid diamide was added [10, 11]. The electrochemical cell was equipped with a graphite anode; a chorine silver reference electrode was connected to the circuit to maintain the constant potential $U = -600$ mV, controlled by Potentiostat IPC-Compact unit.

The uniaxial tension tests were carried out at the rate of 0.2 mm/min at room temperature on LFM-125 universal testing machine. Displacement vector fields of points on the surface of the specimens were recorded simultaneously using double-exposure speckle photography. Decoding procedure of double-speckle images was carried out using ALMEC, a special-purpose equipment developed by ISPMS SB RAS [2, 12]. Thus, all the components of the plastic distortion vector such as local elongation, reduction, shear and rotation could be calculated. Analysis of the deformation localization of the stainless steel was carried out based on the spatial-periodical distribution of local elongation ε_{xx}.

RESULTS AND DISCUSSION

The stress-strain curves obtained for the tempered material and after its hydrogenation in the electrolytic cell were studied [13]. The linear-hardening flow stage was singled out for every deformation diagrams based on the work hardening coefficient θ distribution, as far as within the linear stage $\theta = d\sigma/d\varepsilon = \text{const}$ (Table 1). Hydrogen saturation of tempered steel test samples for 6 and 12 hours resulted in remarkable changes of mechanical properties such as tensile strength and elongation up to the fracture of the specimen, but still every deformation diagram contains a linear work hardening stage.

TABLE 1. Mechanical characteristics of high-chromium stainless steel

	σ_B, MPa	δ, %	Linear hardening stage	
			ε_{ini}	ε_{fin}
Tempered steel	1251	15.3	0.035	0.050
Hydrogenated within 6h	953	12.3	0.034	0.042
Hydrogenated within 12h	922	9.8	0.025	0.037

Using double-exposure speckle photography, the spatial distribution of local elongation of the specimen ε_{xx} observed in the linear hardening stage could be obtained for the tempered state and after electrolytic hydrogenation for 6 and 12 hours, respectively. The sequence of coordinates for each of the localized plastic deformation domains at this stage was approximated by nearly parallel straight lines, see Figs. 2b and 2d, where the slope of the curves enabled the estimation of the velocity of the domains $V_{aw} = \mathrm{d}X/\mathrm{d}t$. The autowave length λ was found from the curve spacing measured along the axis *X*.

Thus, obviously from Fig. 2b and 2d, that the localized-strain patterns in the linear hardening stage where $\theta(\varepsilon) = \mathrm{const}$, are the system of equidistant mobile localized-strain centers with characteristics inherent to a wave process. The autowave velocity and length for the studied states are given in Table 2 to show satisfactory agreement with the universal inversely proportional relation between the macrolocalized plastic-strain autowave velocity and the work-hardening coefficient normalized by the shear modulus of the material [2, 10]. The shape of this dependence ($V_{aw} \sim 1/\theta$) is quite different from the well-known Kolsky waves of plasticity described by the dependence $V_{pl} \sim \sqrt{\theta/\rho}$ (here ρ is density). The distinction between the two dependences above allows concluding that we have discovered a new type of wave processes: self-excited waves of plastic flow. The waves of the new type will be generated in the deforming specimen irrespectively of electrolytic hydrogenation [2, 10–13].

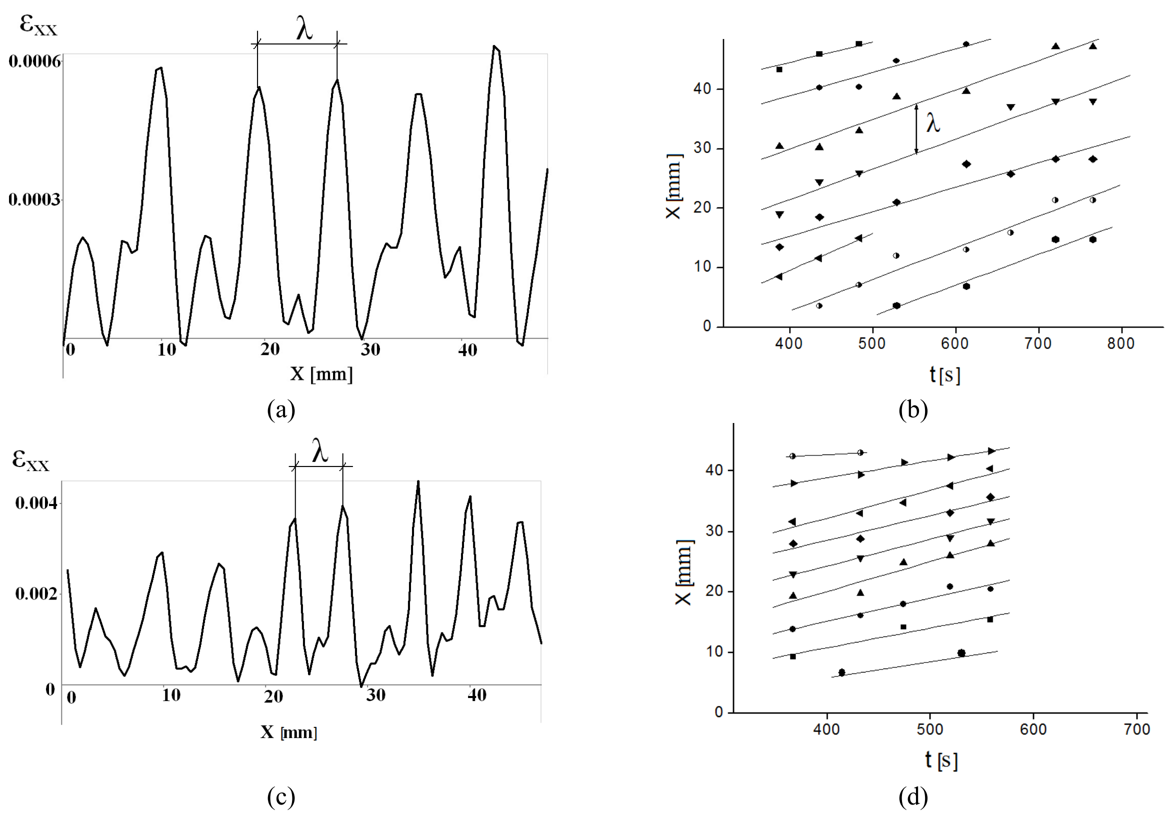

FIGURE 2. (a) Local elongation component ε_{xx} distribution along axis of tension and (b) *X*–*t* diagram of localized plastic deformation domains migration for the tempered steel; (c, d) are the same for the hydrogenated steel during 12 hours

TABLE 2. The characteristics of localized-strain autowaves

	$V_{aw} \times 10^5$, m/s	$\lambda \times 10^3$, m
Tempered steel	5.2±0.9	6.8±1.5
Hydrogenated within 6 h	4.5±0.7	4.4±0.6
Hydrogenated within 12 h	4.0±0.7	4.6±0.5

Using standard statistical processing such as the Student's t-criteria [14], it was determined that for the confidence level α = 0.95, the resulting quantity $|t| \geq t_{\alpha,f}$ is true for the value of the autowave length. This fact suggests that the average λ-values obtained for the tempered and hydrogenated alloys differ significantly.

CONCLUSIONS

The deformation behavior of high-chromium stainless steel subjected to high-temperature tempering and saturated with hydrogen in the three-electrode electrochemical cell under controlled constant cathode potential for 6 and 12 hours was investigated. Hydrogen saturation for 6 hours results in remarkable changes of ultimate stress and total elongation of the material under study. The stress-strain curves of the examined states of stainless steel are characterized by linear work-hardening stage with a constant values of θ. The phase autowave of plasticity occur during the linear stage limits for the tempered steel as well as for the steel after hydrogen saturation.

Comparison of the data for the two conditions (tempered condition and after hydrogenation) of steel showed that the change in the microstructure of hydrogen-saturated tempered steel also affects the plastic strain localization patterns. Hydrogen significantly enhances the localization and changes the quantitative parameters of the macroscopic plastic strain localization: the wave length of autowave plastic strain localization. The mechanism of hydrogen-stimulated plastic strain localization is still under discussion.

ACKNOWLEGMENTS

The work was performed in the frame of the Program of Fundamental Research of State Academies of Sciences for 2013–2020 and was supported in part by the Russian Foundation for Basic Research (project No. 16-08-00385-a).

REFERENCES

1. A. Asharia, A. Beaudoin, and R. Miller, Math. Mech. Sol. **13**, 292–315 (2008).
2. L. B. Zuev and S. A. Barannikova, Int. J. Mech. Sci. **88**, 1–7 (2014).
3. H. Fuchigami, H. Minami, and M. Nagumo, Phil. Mag. Lett. **86**, 21–29 (2006).
4. I. M. Robertson, Eng. Frac. Mech. **68**, 671–692 (2001).
5. J. Sanchez, S. F. Lee, M. A. Martin-Rengel, J. Fullea, C. Andrade, and J. Ruiz-Hervias, Eng. Fail. Anal. **59**, 467–477 (2016).
6. N. Eliaz, A. Shachar, B. Tal, and D. Eliezer, Eng. Fail. Anal. **9**, 167–184 (2002).
7. Y. Liang, P. Sofronis, and N. Aravas, Acta Mater. **51**, 2717–2730 (2003).
8. J. Pelleg, *Mechanical Properties of Materials* (Springer, New York–London–Dordrecht–Heidelberg, 2013).
9. G. E. Totten and M. A. H. Howes, S*teel Heat Treatment Handbook* (Marcel Dekker Inc., New York, Basel, 1997).
10. L. B. Zuev, S. A. Barannikova, M. V. Nadezhkin, and V. A. Mel'nichuk, Techn. Phys. Lett. **37**, 793–796 (2011).
11. S. A. Barannikova, A. G. Lunev, M. V. Nadezhkin, and L. B. Zuev, Adv. Mater. Res. **880**, 42–47 (2014).
12. L. B. Zuev, V. I. Danilov, S. A. Barannikova, and V. V. Gorbatenko, Phys. Wav. Phen. **17**, 66–75 (2009).
13. A. V. Bochkareva, S. A. Barannikova, A. G. Lunev, Yu. V. Li, and L. B. Zuev, in *IEEE Proc. Int. Conf. Mechanical Engineering, Automation and Control Systems MEACS*, 1–3 (2015).
14. D. J. Hudson, *Lectures on Elementary Statistics and Probability* (Geneva: CERN, 1963).